The magnetization reversal behaviour for $SmCo_{6.8}Zr_{0.2}$ and $SmCo_{6.8}Zr_{0.2}/\alpha$-(Fe,Co) nanocrystalline magnets at low temperature*

Liu Zhuang(刘 壮)[a)b)†], Chen Ren-Jie(陈仁杰)[a)], Li Dong(李 东)[a)], and Yan Ar-Ru(闫阿儒)[a)]

[a)] *Zhejiang Province Key Laboratory of Magnetic Materials and Application Technology, Ningbo Institute of Material Technology & Engineering, Chinese Academy of Sciences, Ningbo* 315201, *China*

[b)] *Institute of Solid State Physics, Chinese Academy of Sciences, Hefei* 230031, *China*

(Received 9 October 2009; revised manuscript received 2 November 2009)

This paper reports that the $SmCo_{6.8}Zr_{0.2}$ nanocrystalline permanent magnets and $SmCo_{6.8}Zr_{0.2}/\alpha$-(Fe,Co) nanocomposite permanent magnets are successfully produced by mechanical alloying and subsequently annealing at 700 °C for 10 minutes. The x-ray diffraction results show that the phase structure of $SmCo_{6.8}Zr_{0.2}$ nanocrystalline permanent magnets is composed of $SmCo_7$ phase and $SmCo_{6.8}Zr_{0.2}/\alpha$-(Fe,Co) nanocomposite permanent magnets is composed of $SmCo_7$ and α-(Fe,Co) phases. The mechanism of magnetization reversal is mainly controlled by inhomogeneous domain wall pinning in $SmCo_{6.8}Zr_{0.2}$ and $SmCo_{6.8}Zr_{0.2}/\alpha$-(Fe,Co) magnets. The inter-grain exchange interaction at low temperature is investigated, which shows that the inter-grain exchange interaction of $SmCo_{6.8}Zr_{0.2}/\alpha$-(Fe,Co) magnets increases greatly by the decrease of the measured temperature. According to $\Delta m_{\rm irr}$–$H/H_{\rm cj}$, $\Delta m_{\rm rev}$–$H/H_{\rm cj}$ and $\chi_{\rm irr}$–$H/H_{\rm cj}$ curves at room temperature and 100 K, the changes of irreversible and reversible magnetization behaviours of $SmCo_{6.8}Zr_{0.2}$ and $SmCo_{6.8}Zr_{0.2}/\alpha$-(Fe,Co) magnets with the decreasing temperature are analysed in detail. The magnetic viscosity and the activation volume of $SmCo_{6.8}Zr_{0.2}$ and $SmCo_{6.8}Zr_{0.2}/\alpha$-(Fe,Co) magnets at different temperatures are also studied.

Keywords: nanocrystalline magnets, coercivity mechanism, inter-grain exchange coupling, magnetization reversal behaviour

PACC: 7560E, 7550V, 7500

1. Introduction

Nanocomposite magnets have attracted much interests from researchers for the possible highest maximum magnetic energy $(BH)_{\rm max}$. Remanence enhancement has been observed in the nanocrystalline magnets due to the inter-grain exchange interaction (IGEI) of the nanograins. Many attempts have been made to investigate physical essentials in a single-phase nanocrystalline permanent magnet (PM) and the nanocomposite PM.[1−4] Although a single-phase demagnetization behaviour with high remanence and coercivity has been realized in the simulations for isotropic nanocomposite PM, the calculated remanence and coercivity are much larger than those in experiments.[5−7] The huge difference between the experimental results and the theoretical results indicates that the theory about nanocomposite magnets is uncertain and the magnetic reversal behaviour should be studied in detail.

In a single-phase nanocrystalline PM, the coercivity is usually larger than the remanence.[1,8,9] However, for most isotropic nanocomposite permanent magnets (PMs),[10,11] the value of coercivity ($<$ 0.56 MA/m) is lower than that of remanence ($>$ 1.0 T), which results in a low value of $(BH)_{\rm max}$. Thus, enhancing coercivity becomes the key to obtaining high prominence PMs. The $SmCo_7$ alloys have excellent permanent magnetic properties, which is a requirement for a high coercivity of nanocomposite PMs. Considering the difference of temperature dependence of magnetic properties between soft and hard phases, we recognize that the research of magnetization behaviours at different temperatures should give more information about the magnetization mech-

*Project supported by the Natural Science Foundation of Zhejiang Province of China (Grant No. Y407174), Major Scientific and Technological Special Fund of Zhejiang Province of China (Grant No. 2007C11046) and the National Basic Research Program of China (Grant No. 2010CB934601).

†Corresponding author. E-mail: zliu@nimte.ac.cn

© 2010 Chinese Physical Society and IOP Publishing Ltd

anism of nanocrystalline PMs. In this work, we prepared the single-phase nanocrystalline PM $SmCo_7$ and the nanocomposite PM $SmCo_7/\alpha$-(Fe,Co) by mechanically alloying and subsequently annealing and comparatively studying their magnetization behaviours at different temperatures.

2. Experiment

The $SmCo_{6.8}Zr_{0.2}$ alloy was prepared by arc melting with an excess Sm of 10 wt% to compensate the weight loss due to Sm evaporation. The alloy was melted four times to ensure homogeneity. The as-cast alloy was crushed into coarse powder with typical sizes less than 180 μm and the powder was mechanically milled for 10 hours under argon atmosphere by using a high-energy Spex 8000 mill with a ratio of powder to ball of 1:2. The as-milled powder was subsequently annealed at 700 °C for 10 minutes and nanocrystalline magnets $SmCo_{6.8}Zr_{0.2}$ (SZ) were obtained. In order to produce the $SmCo_{6.8}Zr_{0.2}/\alpha$-(Fe,Co) nanocomposite PM (SZ/F), 5 wt% α–Fe powder with particle sizes less than 10 μm was mixed with the crushed powder of $SmCo_{6.8}Zr_{0.2}$ and then the mixture was milled and subsequently annealed under the same condition as the sample SZ. The magnetic properties were measured with the resin-bonded magnets made with the nanocrystalline powder.

The crystal structures were determined by Bruker AXS x-ray diffraction (XRD) with Co Kα radiation. The magnetic properties of resin-boned magnets produced from the powder were measured by using a Quantum Design model 9 Physical Property Measurement System (PPMS-9) with a maximum field of 9 T at room temperature. No correction was made for the demagnetization field effect.

3. Results and discussion

The XRD patterns of $SmCo_{6.8}Zr_{0.2}$ (SZ) and $SmCo_{6.8}Zr_{0.2}/\alpha$-(Fe,Co) nanocomposite PM (SZ/F) with 5 wt% α-Fe are shown in Fig. 1. According to Fig. 1, the phase structure of sample SZ mainly consisted of $TbCu_7$ type $SmCo_7$ phase while sample SZ/F consisted of $SmCo_7$ and α-(Fe,Co) phase. From the analysis of XRD patterns, the single-phase nanocrystalline PM and the two-phase nanocomposite PM are successfully produced by mechanical milling.

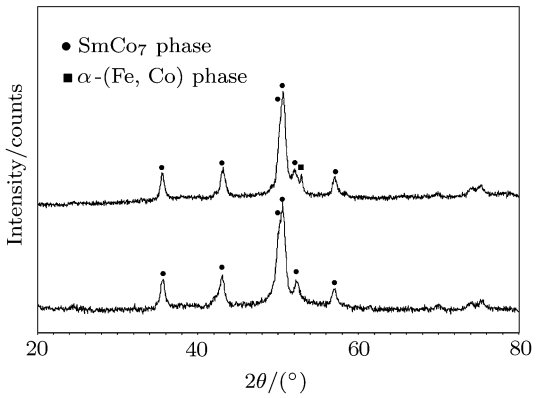


Fig. 1. The XRD pattern of $SmCo_{6.8}Zr_{0.2}$ and $SmCo_{6.8}Zr_{0.2}/\alpha$-(Fe,Co) nanomagnets.

The minor hysteresis loops of SZ and SZ/F are measured. Figure 2 shows the field dependence of the reduced remanence ($m_r(H) = M_r(H)/M_s$) and coercivity ($H_c(H)/H_{cj}$) which are obtained from the minor hysteresis loops. Here the remanence $M_r(H)$ and coercivity $H_c(H)$ are acquired after application and subsequently turn to $-H$, M_s and H_{cj} are the saturated magnetization and coercivity determined by the major demagnetization curve. According to Fig. 2, the $m_r(H)$ and $H_c(H)/H_{cj}$ of SZ and SZ/F are low at $H^{max}/H_{cj} < 0.9$. However, they grow rapidly after a critical field ($H^{max}/H_{cj} \approx 0.9$), which are the typical features of domain wall pinning.[12,13] Moreover, the low values of m_r (< 0.5) even at $H^{max}/H_{cj} \approx 1.3$ suggest the coercivity mechanism of SZ and SZ/F is different from the ordinary model of domain wall pinning, for which the value of $m_r > 0.5$ will be soon reached after $H^{max}/H_{cj} > 0.9$.[14] So it indicates that the mechanism of magnetic reversal is mainly controlled by inhomogeneous domain wall pinning in SZ and SZ/F, which could come from the imperfections at the hard–hard and the hard–soft interface.

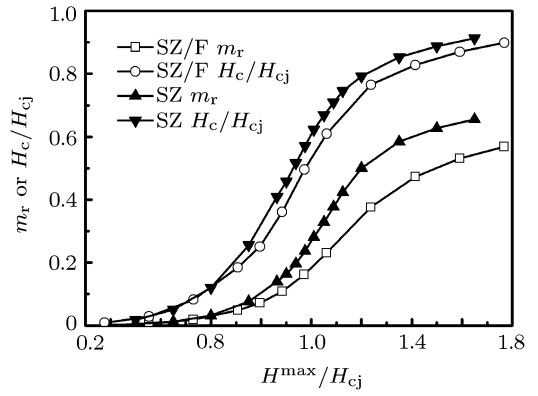


Fig. 2. The field dependence of the reduced remanence m_r ($M_r(H)/M_s$) and coercivity (H_c/H_{cj}) obtained from the minor hysteresis loops of SZ and SZ/F powders.

As can also be seen from Fig. 2, the field dependence of $m_r(H)$ and $H_c(H)/H_{cj}$ of SZ and SZ/F are the same as those at the field H/H_{cj} less than 0.6, but the values of $m_r(H)$ and $H_c(H)/H_{cj}$ of SZ are greater than those of SZ/F as further increase of the field. This indicates that the single phase nanocrystalline PM SZ is magnetized more easily than nanocomposite PM SZ/F, which is due to the difference between soft and hard phases results in an enhancement of domain wall pinning in the sample SZ/F.

Figure 3 shows the dependence of reduced remanence $m_r(M_r/M_s)$ of SZ and SZ/F on temperature. It can be seen that all the m_r values of SZ and SZ/F are larger than 0.5, i.e. the enhancement of remanence, which indicates a strong exchange interaction in SZ and SZ/F nanocrystalline magnets.[8] It also can be seen that the m_r decreases with the drop in temperature. And the decreasing rate of m_r for SZ/F is a little smaller than that for SZ, which is due to the competition of anisotropy energy and exchange coupling energy. This is consistent with the results of $Pr_2Fe_{14}B$ and $Pr_2Fe_{14}B/\alpha$-Fe ribbons.[15]

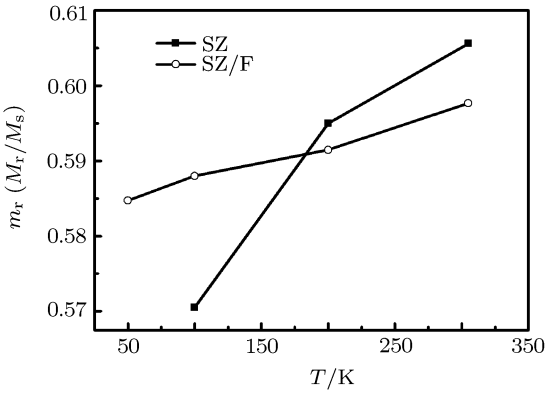


Fig. 3. The dependence of reduced remanence m_r of SZ and SZ/F nanocrystalline magnets on temperature.

The Henkel–Plot curve is usually used to analyse the IGEI in nanocrystalline PMs. The expression of a Henkel plot is as follows:[16] $\delta m(H) = [M_d(H) - M_r + 2M_r(H)]/M_r$. Positive values of $\delta m(H)$ are due to exchange coupling interaction promoting the magnetization state, while negative values of $\delta m(H)$ are caused by magnetic dipole interaction tending to assist magnetization reversal. As shown in Fig. 4, positive $\delta m(H)$ values indicate a strong IGEI in the SZ and SZ/F samples, and the peak value of $\delta m(H)$ for SZ is higher than that of SZ/F, which indicates that the IGEI of SZ is stronger than SZ/F. Furthermore, it also can be seen that the maximum positive $\delta m(H)$ value for SZ at room temperature (RT) and 100 K is almost the same while it increases a lot for SZ/F, implying that the IGEI is not only related to the microstructure of hard and soft phase but also the magnetocrystalline anisotropy constant K and exchange constant A of hard and soft phase. In order to improve the coercivity of nanocomposite PM, an appropriate K and A of hard and soft phase is necessary to achieve the strongest IGEI.

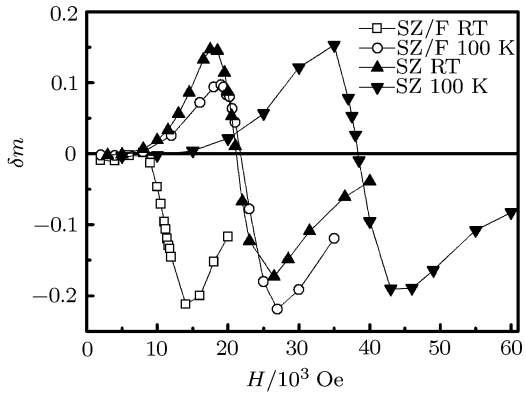


Fig. 4. Variation of $\delta m = \{M_d(H) + 2M_r(H) - M_r\}/M_r$ with the applied magnetic field for SZ and SZ/F measured at RT and 100 K, 1 Oe=1 Gb/cm.

In order to thoroughly understand the process of magnetization reversal of SZ and SZ/F at RT and low temperature, nucleation fields H_{no} and the reversible magnetization m_{rev} are taken into account. This quantity is defined as the difference in magnetization obtained when traversing the recoil curve, starting from a point on the demagnetization curve for a given field and terminating on the recoil curve at zero field.[17] The reversible portion Δm_{rev} is defined as the reversible magnetization normalized with respect to the remanence M_r and the irreversible portion is defined as $\Delta m_{irr} = [M_r - M_d(H)]/2M_r$, where $M_d(H)$ is the DC field demagnetization remanence acquired after saturation magnetized in one direction and subsequent application of a DC field H in the opposite direction. Figure 5(a) shows the Δm_{irr}–H/H_{cj} curves for SZ and SZ/F at RT and 100 K. It can be seen that little change of Δm_{irr} is observed for SZ sample at RT and 100 K; while a higher irreversible portion of SZ/F at RT by contrast with that at 100 K is observed at lower reversal field of $H/H_{cj} < 1$. The Δm_{irr}–H/H_{cj} curves have been explained by a one-dimensional purely inhomogeneous magnetization rotation model.[18] No magnetization reversal occurs when the reversal field H increases from 0 to a certain value H_n. When H increases further to a certain value $H_1 = H_n/\cos\theta_1$, all regions with

$0 \leq \theta \leq \theta_1$ have reversed, where θ is the angle between reversible magnetic field and the easy magnetization direction of individual single-domain grain. According to Fig. 5(a), it can be concluded that more hard grains switch together with the soft grains in the field H_n with the decrease of the temperature, implying that the IGEI of SZ/F measured at 100 K is stronger than that of SZ/F at RT. This feature can also be observed in the χ_{irr} $(d\Delta m_{irr}/dH) - H/H_{cj}$ curves for SZ and SZ/F at RT and 100 K shown in Fig. 5(c).

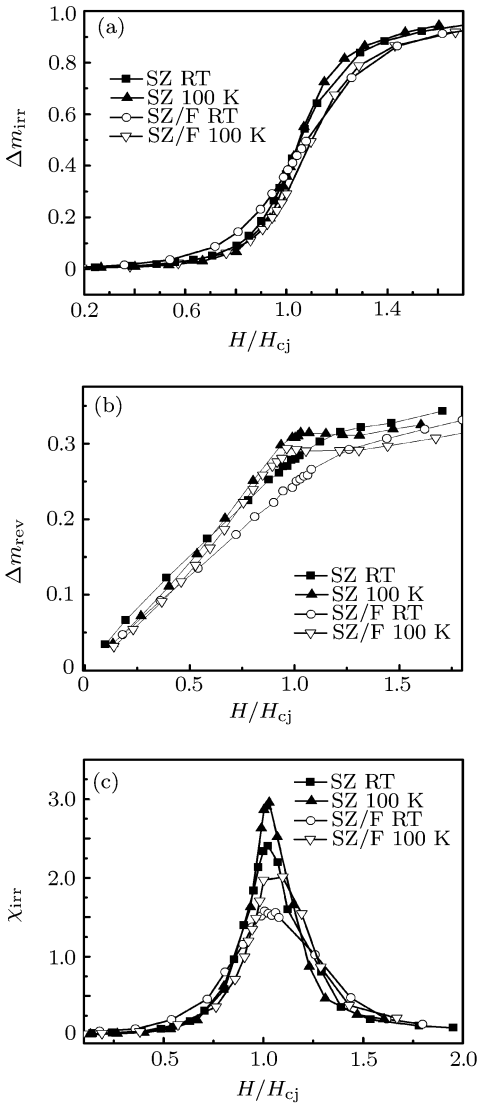


Fig. 5. (a) Irreversible reduced portion $\Delta m_{irr} = [M_r - M_d(H)]/2M_r$, (b) reversible reduced portion $\Delta m_{rev} = [M_d(H) - M(H)]/M_r$, and (c) irreversibility susceptibility $\chi_{irr} = d\Delta m_{irr}/dH$ vs. the reverse field divided by the coercivity for SZ and SZ/F samples at RT and 100 K.

The peak value of the SZ/F sample at 100 K shows a larger H/H_{cj} value than that of SZ/F at RT. Furthermore, the derivative $d\Delta m_{irr}/dH = f(H_n)$ can be defined as the distribution function of critical fields H_n for reversal of irreversible magnetization.[5] The nucleation field H_{no} for irreversible magnetization can be obtained from the maximum of $\chi_{irr} - H/H_{cj}$. The irreversible nucleation field H_{no} has been achieved for SZ and SZ/F at RT and 100 K, which are all larger than their coercivity. According to the model given by Kneller and Hawig,[5] when the size of soft phase b_m is equal to the critical size of soft phase b_{cm} which will give the largest coercivity, it will make $H_{cj} > H_{no}$. However, if $b_m \gg b_{cm}$, it will make $H_{cj} < H_{no}$. It can be concluded that the size of α-(Fe,Co) phase for SZ/F is larger than the critical size ofthe soft phase. Thus, decreasing the size of the α-(Fe,Co) phase is necessary to further improve the coercivity of nanocomposite PM. The irreversible portion at the field equal to nucleation field for the SZ/F at 100 K is around 44%, which is a little larger than that for SZ/F at RT (41%). It appears that stronger IGEI should be expected for SZ/F at 100 K by contrast with SZ/F at RT, which is consistent with the results of the Henkel–Plot curve (Fig. 4). The reversible portion Δm_{rev} as a function of H/H_{cj} is given in Fig. 5(b) for comparison. The maximum value of Δm_{rev} for SZ/F is a little smaller than that for SZ at RT, which could be attributed to the existence of the α-(Fe,Co) soft phase in the SZ/F sample. This is similar to the results of the $Sm_2Fe_{15}Ga_2C_x/\alpha$-Fe[19] system and the $Pr_{12}Fe_{82}B_6$[20] ribbons. It also can be seen that a higher reversible proportion is observed in SZ/F at 100 K than that in SZ/F at RT for a given reverse field. It also suggests that SZ/F at 100 K maintains a stronger exchange coupling between interphases contrasted with SZ/F at RT, similar to the result of Δm_{irr}–H/H_{cj} curves.

The magnetic viscosity arises from the thermal activation of magnetization reversal for overcoming energy barriers. Thermal activation enables magnetization irreversible reversal, thus magnetic viscosity is expected to give some information on the irreversibility of the nanocrystalline PMs. Viscosity constant S is obtained by using the following equation:[21]

$$J(t) = J_0 - S\ln(t + t_0), \tag{1}$$

where $J(t)$ is the magnetization changing with time at a fixed applied field, t is the time since the applied field is held, and J_0 and t_0 are constants. The viscosity coefficient $S = -dJ/d\ln t$ can be obtained from Eq. (1). The RT magnetic viscosity coefficient S and irreversible susceptibility χ_{irr} of SZ/F are shown in Fig. 6(a) as a function of the reverse field H. Both

the $\chi_{\rm irr}$ and the S curves exhibit maxima at approximately the same reverse field around coercivity. For the hard–soft nanocomposite magnet, the irreversibility is primarily from the hard phase. Therefore, the time-dependent changes of magnetization should be primarily attributed to the $SmCo_7$ hard phase. Figure 6(b) shows the change of magnetic viscosity coefficient S with the field at different temperatures. The value of S decreases with the drop in temperature. And from the intensity of S at different temperatures, it also can be seen that $S^{\rm max}$ declines with the drop in temperature, which should be related to the weak influence of thermal disturbance with the drop in temperature. It is consistent with the result of PrFeB/α-Fe nanocrystal ribbons.[16]

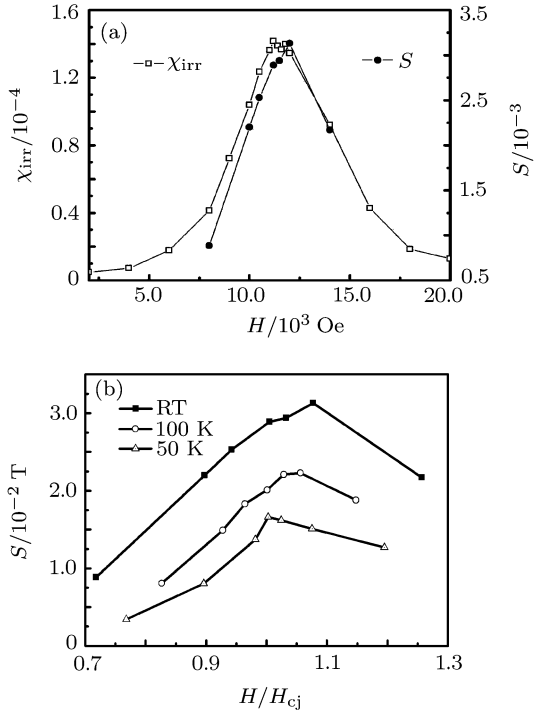


Fig. 6. (a) The magnetic viscosity coefficient S and irreversible susceptibility $\chi_{\rm irr}$ of SZ/F sample as functions of the reverse field H at RT. (b) The magnetic viscosity coefficient S as a function of $H/H_{\rm cj}$ at different temperatures.

The activation volume can provide information about the magnetic reversal behaviour in magnets. According to Gaunt,[22] the activation volume can be defined as $V = K_{\rm B}T/H_{\rm f}M_{\rm s}$ for the typical domain wall pinning controlled magnets, where $H_{\rm f} = S/X_{\rm irr}$ is known as the fluctuation field and $H_{\rm f}$ is constant at a given temperature. Figure 7 shows the activation volume of SZ and SZ/F at different temperatures. The activation volumes, $V = 1.9 \times 10^{-18}$ cm^3 and 1.1×10^{-18} cm^3 for SZ/F and SZ respectively, have been estimated with fields around the coercivity at RT. The activation volume of SZ/F measured at RT is roughly consistent with the cellular microstructure of $Sm(Co,Fe,Cu,Zr)_z$ primarily consisting of the Sm_2Co_{17} phase and the $SmCo_5$ phase.[23] It also can be seen that the activation volumes of SZ and SZ/F are decreasing with the drop in temperature. From the decreasing rate of activation volume with temperature, it can be seen that the activation volume of SZ/F decreases more quickly than that of SZ, which could be related to the IGEI of SZ and SZ/F. The IGEI makes the moment of a grain parallel to the neighbouring ones, which means stronger IGEI will make the moment reversal by the thermal disturbance more difficult. Thus, it could produce a smaller reversal region or the activation volume at a certain field. And from the $\delta m(H)$ curves of SZ and SZ/F at RT and 100 K, it can be seen that the IGEC of SZ/F increases more quickly than that of SZ with temperature decreasing from RT to 100 K, which could lead to the different decreasing rate of the activation volumes for SZ and SZ/F.

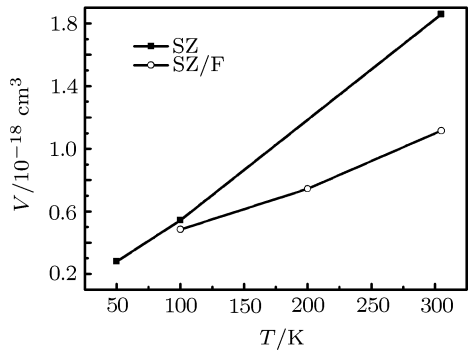


Fig. 7. The activation volumes of SZ and SZ/F at different temperatures.

4. Conclusions

The mechanism of magnetic reversal is mainly controlled by inhomogeneous domain wall pinning in SZ and SZ/F. The reduced remanence decreases with the decrease in temperature. According to the $\delta m(H)$–H curves of SZ and SZ/F at RT and 100 K, IGEI of SZ/F is greatly increased with temperature decreasing from RT to 100 K while a small change of IGEI is observed for SZ. From the analysis of the $\Delta m_{\rm irr}$–$H/H_{\rm cj}$ for SZ and SZ/F, it indicates that more hard grains switch together with the soft grains in

the field $H_{\rm n}$ with decreasing temperature due to the stronger IGEI for SZ/F at 100 K. Consistent results are also obtained from the analysis of the reversible portion $\Delta m_{\rm rev}$–$H/H_{\rm cj}$ curves for SZ and SZ/F at RT and 100 K. The irreversible nucleation fields $H_{\rm no}$ for SZ and SZ/F at RT and 100 K are all larger than their coercivity. Finally, the activation volumes of SZ and SZ/F decrease with the drop in temperature. And the activation volumes of SZ/F decrease more quickly than that of SZ, which could be related to the IGEI.

References

[1] Goll D, Seeger M and Kromüller H 1998 *J. Magn. Magn. Mater.* **185** 49

[2] Yan A, Bollero A, Gutfleisch O and Muller K H 2002 *J. Appl. Phys.* **91** 2192

[3] Zhang J, Zhang S Y, Zhang H W, Shen B G and Li B H 2001 *J. Appl. Phys.* **89** 2857

[4] Chen R J, Zhang H W, Shen B G, Yan A R and Chen D L 2009 *Chin. Phys.* B **18** 2582

[5] Kneller E F and Hawig R 1991 *IEEE Trans. Magn.* **27** 3588

[6] Skomski R and Coey J M D 1993 *Phys. Rev.* B **48** 15812

[7] Skomski R 1994 *J. Appl. Phys.* **76** 7059

[8] Hadjipanayis G C 1999 *J. Magn. Magn. Mater.* **200** 373

[9] Zhang H W, Rong C B, Zhang J, Zhang S Y and Shen B G 2002 *Phys. Rev.* B **66** 184436

[10] Manaf A, Buckley R A and Davies H A 1993 *J. Magn. Magn. Mater.* **128** 302

[11] Zhang H W, Zhang S Y, Shen B G and Lin C 1999 *J. Appl. Phys.* **85** 4660

[12] Pinkerton F E and Van Wingerden D J 1996 *J. Appl. Phys.* **6** 3685

[13] Liu J F, Luo H L and Wan J 1992 *J. Pediatr. (St. Louis).* **25** 1238

[14] Buschow K H J 1991 *Rep. Prog. Phys.* **54** 1123

[15] Zhang H W, Zhao T Y, Rong C B, Zhang S Y, Han B S and Shen B G 2003 *J. Magn. Magn. Mater.* **267** 224

[16] Kelly P E, Grady K O, Mayo P I and Chantrell R W 1989 *IEEE Trans. Mag.* **25** 3881

[17] Goll D, Kronmüller H and Stadelmaier H H 2004 *J. Appl. Phys.* **96** 6534

[18] Ferguson G B, Grady K O, Popplewell J and Chantrell R W 1989 *IEEE Trans. Magn.* **25** 3449

[19] Cheng Z H, Zhan J X and KronmÜller H 2003 *Phys. Rev.* B **68** 14441

[20] Zhang H W, Zhang S Y, Shen B G, Goll D and Kronmuller H 2001 *Chin. Phys.* **10** 1169

[21] Singleton E W and Hadjipanaysis G C 1990 *J. Appl. Phys.* **67** 4759

[22] Gaunt P 1986 *J. Appl. Phys.* **59** 4129

[23] Panagiotopoulos I, Gjoka M and Niarchos D 2002 *J. Appl. Phys.* **92** 7693